Available online at www.sciencedirect.com
SCIENCE DIRECT®
International Journal of Solids and Structures 42 (2005) 4338–4351
INTERNATIONAL JOURNAL OF SOLIDS and STRUCTURES
www.elsevier.com/locate/ijsolstr

Numerical solution of the Cauchy problem for steady-state heat transfer in two-dimensional functionally graded materials

Liviu Marin *

School of Earth and Environment, Environment Centre, University of Leeds, Woodhouse Lane, Leeds LS2 9JT, UK

Received 20 December 2004
Available online 9 March 2005

Abstract

The application of the method of fundamental solutions to the Cauchy problem for steady-state heat conduction in two-dimensional functionally graded materials (FGMs) is investigated. The resulting system of linear algebraic equations is ill-conditioned and, therefore, regularization is required in order to solve this system of equations in a stable manner. This is achieved by employing the zeroth-order Tikhonov functional, while the choice of the regularization parameter is based on the L-curve method. Numerical results are presented for both smooth and piecewise smooth geometries. The convergence and the stability of the method with respect to increasing the number of source points and the distance between the source points and the boundary of the solution domain, and decreasing the amount of noise added into the input data, respectively, are analysed.

Keywords: Meshless method; Method of fundamental solutions; Cauchy problem; Functionally graded materials (FGMs); Regularization; Inverse problem

1. Introduction

In recent years, functionally graded materials (FGMs) have been introduced and applied in the development of structural components subject to non-uniform service requirements. FGMs possess continuously varying microstructure and mechanical and/or thermal properties. These materials are essentially

* Corresponding author. Present address: School of Mechanical, Materials and Manufacturing Engineering, The University of Nottingham, University Park, Nottingham NG7 2RD, UK. Tel.: +44 113 343 6744; fax: +44 113 343 6716.
E-mail addresses: liviu@env.leeds.ac.uk, liviu.marin@nottingham.ac.uk

0020-7683/$ - see front matter © 2005 Elsevier Ltd. All rights reserved.
doi:10.1016/j.ijsolstr.2005.01.005

two-phase particulate composites, e.g. ceramic and metallic alloy phases, synthesized such that the composition of each constituent changes continuously in one direction, to yield a predetermined composition profile, see e.g. Suresh and Mortensen (1998). Although the initial application of FGMs was to synthesize thermal barrier coatings for space applications, see e.g. Hirano et al. (1990), later investigations uncovered a wide variety of potential applications, such as nuclear fast breeder reactors, see e.g. Igari et al. (1990), graded refractive index materials in audio–video disks, see e.g. Koike (1992) piezoelectric and thermoelectric devices, see e.g. Osaka et al. (1990), Tani and Liu (1993) and Watanabe et al. (1993), dental and medical implants, see e.g. Oonishi et al. (1994), thermionic converters, see e.g. Desplat (1996), etc. However, for the sake of the physical explanation, we will refer in this study to the steady-state heat conduction problem for FGMs.

In most boundary value problems in heat transfer, the thermal equilibrium equation has to be solved with the appropriate initial and boundary conditions for the temperature and/or normal heat flux, i.e. Dirichlet, Neumann or mixed boundary conditions. These problems are called direct problems and their existence and uniqueness have been well established, see for example Hadamard (1923). However, there are other engineering problems which do not belong to this category. For example, the thermal conductivities and/or the heat sources are unknown, the geometry of a portion of the boundary is not determined or the boundary conditions are incomplete, either in the form of underspecified and overspecified boundary conditions on different parts of the boundary or the solution is prescribed at some internal points in the domain. These are inverse problems, and it is well known that they are generally ill-posed, i.e. the existence, uniqueness and stability of their solutions are not always guaranteed, see e.g. Hadamard (1923).

A classical example of an inverse problem in steady-state heat transfer is the Cauchy problem in which both temperature and normal heat flux boundary conditions are prescribed only on a part of the boundary of the solution domain, whilst no information is available on the remaining part of the boundary. This inverse boundary value problem has been studied by many authors for heat conduction in isotropic materials, see e.g. Ingham and Yuan (1994), Lesnic et al. (1997) and Hào and Lesnic (2000), anisotropic media, see Mera et al. (2000, 2002), and heat conduction in fins, see Marin et al. (2003a,b). However, to our knowledge, the Cauchy problem for steady-state heat conduction in two-dimensional anisotropic FGMs has not been investigated as yet. In addition, the numerical solution to this inverse problem is approached by employing the method of fundamental solution (MFS), originally introduced by Kupradze and Aleksidze (1964) and then applied for solving numerically a wide variety of boundary value problems, see e.g. Karageorghis and Fairweather (1987), Fairweather and Karageorghis (1998), Poullikkas et al. (1998a,b, 2001, 2002), Berger and Karageorghis (1999, 2001), Karageorghis (2001) and Ramachandran (2002). The advantages of the MFS over domain discretisation methods, such as the finite-difference (FDM) and the finite element methods (FEM), are very well documented, see Fairweather and Karageorghis (1998). Moreover, the MFS has all the advantages of boundary methods, such as the boundary element method (BEM), as well as several advantages over other boundary methods. For example, the MFS does not require an elaborate discretisation of the boundary, integrations over the boundary are avoided, the solution in the interior of the domain is evaluated without extra quadratures, its implementation is very easy and only little data preparation is required.

In this paper, we extend the method proposed by Marin and Lesnic (2004, 2005) and Marin (in press, in press) for solving numerically the Cauchy problem in two- and three-dimensional isotropic elastostatics and Helmholtz-type equations, respectively, to the steady-state heat conduction in two-dimensional anisotropic FGMs. The MFS discretised system of equations corresponding to the Cauchy problem for steady-state heat conduction in two-dimensional anisotropic FGMs is ill-conditioned and hence it is solved by employing the zeroth-order Tikhonov regularization method, see e.g. Tikhonov and Arsenin (1986), whilst the choice of the regularization parameter is based on the L-curve criterion, see Hansen (2001). Three examples for steady-state heat transfer in two-dimensional anisotropic FGMs involving smooth and piecewise smooth geometries are investigated and the convergence and stability of the method with respect to the

location and the number of source points and the amount of noise added into the Cauchy input data, respectively, are analysed.

2. Mathematical formulation

Consider an open bounded domain $\Omega \subset \mathbb{R}^2$ occupied by an exponentially graded anisotropic solid and assume that Ω is bounded by a piecewise smooth curve $\Gamma = \partial\Omega$, such that $\Gamma = \Gamma_1 \cup \Gamma_2$, where $\Gamma_1, \Gamma_2 \neq \emptyset$ and $\Gamma_1 \cap \Gamma_2 = \emptyset$. The thermal conductivities of this material can be expressed as, see Berger et al. (in press),

$$k_{ij}(\boldsymbol{x}) = K_{ij} \exp(2\boldsymbol{\beta} \cdot \boldsymbol{x}), \quad \boldsymbol{x} \in \Omega, \quad i,j = 1,2, \tag{1}$$

where the constant real or pure imaginary vector $\boldsymbol{\beta} = (\beta_1, \beta_2)$ characterises the direction and the magnitude of the variation and the matrix $\mathbb{K} = (K_{ij})_{1 \leqslant i,j \leqslant 2}$ is symmetric and positive-definite. It should be noted that $\mathbb{K} = (\delta_{ij})_{1 \leqslant i,j \leqslant 2}$ in the case of an isotropic material, where δ_{ij} is the Kronecker delta tensor. Then the heat flux in the solid is expressed as

$$\varphi_i(\boldsymbol{x}) = -k_{ij}(\boldsymbol{x}) \partial_j T(\boldsymbol{x}), \quad \boldsymbol{x} \in \Omega, \quad i = 1,2, \tag{2}$$

where $T(\boldsymbol{x})$ represents the temperature at $\boldsymbol{x} \in \Omega$, $\partial_j \equiv \partial/\partial x_j$ and the customary standard Einstein notation for summation over repeated indices is used. On using Eqs. (1) and (2), the Fourier law in the absence of heat sources, namely,

$$\partial_i \varphi_i(\boldsymbol{x}) = 0, \quad \boldsymbol{x} \in \Omega, \tag{3}$$

can be expressed in terms of the temperature, T, as

$$-\left(K_{ij} \partial_i \partial_j T(\boldsymbol{x}) + 2\beta_i K_{ij} \partial_j T(\boldsymbol{x})\right) \exp(2\beta \cdot \boldsymbol{x}) = 0, \quad \boldsymbol{x} \in \Omega. \tag{4}$$

We now let $\boldsymbol{n}(\boldsymbol{x})$ be the unit outward normal vector at Γ and $\Phi(\boldsymbol{x})$ be the normal heat flux at a point $\boldsymbol{x} \in \Gamma$ defined by

$$\Phi(\boldsymbol{x}) = n_i(\boldsymbol{x}) \varphi_i(\boldsymbol{x}), \quad \boldsymbol{x} \in \Gamma. \tag{5}$$

In the direct problem formulation, the knowledge of the temperature and/or normal heat flux on the whole boundary Γ gives the corresponding Dirichlet, Neumann, or mixed boundary conditions which enables us to determine the temperature in the solution domain Ω. If it is possible to measure both the temperature and the normal heat flux on a part of the boundary Γ, say Γ_1, then this leads to the mathematical formulation of an inverse problem consisting of Eq. (4) and the boundary conditions

$$T(\boldsymbol{x}) = \widetilde{T}(\boldsymbol{x}), \quad \Phi(\boldsymbol{x}) = \widetilde{\Phi}(\boldsymbol{x}), \quad \boldsymbol{x} \in \Gamma_1, \tag{6}$$

where $\widetilde{T}$ and $\widetilde{\Phi}$ are prescribed functions. In the above formulation of the boundary conditions (6), it can be seen that the boundary Γ_1 is overspecified by prescribing both the temperature $T|_{\Gamma_1} = \widetilde{T}$ and the normal heat flux $\Phi|_{\Gamma_1} = \widetilde{\Phi}$, whilst the boundary Γ_2 is underspecified since both the temperature $T|_{\Gamma_2}$ and the normal heat flux $\Phi|_{\Gamma_2}$ are unknown and have to be determined. This problem, termed the Cauchy problem, is much more difficult to solve both analytically and numerically than the direct problem, since the solution does not satisfy the general conditions of well-posedness. Although the problem may have a unique solution, it is well known, see e.g. Hadamard (1923), that this solution is unstable with respect to small perturbations in the data on Γ_1. Thus the problem is ill-posed and we cannot use a direct approach, such as the Gauss elimination method, in order to solve the system of linear equations which arises from the discretisation of the partial differential equations (4) and the boundary conditions (6). Therefore, regularization methods are required in order to solve accurately the Cauchy problem for anisotropic FGMs.

3. Method of fundamental solutions

The fundamental solution G of the heat balance equation (4) for two-dimensional anisotropic FGMs is given by, see e.g. Clements and Budhi (1999) and Berger et al. (in press),

$$G(\boldsymbol{x},\boldsymbol{y}) = -\frac{K_0(\kappa R)}{2\pi\sqrt{\det \mathbb{K}}} \exp\{-\boldsymbol{\beta}\cdot(\boldsymbol{x}+\boldsymbol{y})\}, \quad \boldsymbol{x}\in\overline{\Omega}, \quad \boldsymbol{y}\in\mathbb{R}^2\setminus\overline{\Omega}, \tag{7}$$

where $\boldsymbol{y}$ is a source point, K_0 is the modified Bessel function of the second kind of order zero, $\kappa = \sqrt{\beta\cdot\mathbb{K}\beta}$, $R = R(\boldsymbol{x},\boldsymbol{y}) = \sqrt{\boldsymbol{r}\cdot\mathbb{K}^{-1}\boldsymbol{r}}$ and $\boldsymbol{r} = \boldsymbol{r}(\boldsymbol{x},\boldsymbol{y}) = \boldsymbol{x}-\boldsymbol{y}$. It should be noted that the fundamental solution for two-dimensional isotropic FGMs has been obtained by Gray et al. (2003).

The main idea of the MFS consists of the approximation of the temperature in the solution domain by a linear combination of fundamental solutions with respect to M source points $\boldsymbol{y}_j$ in the form

$$T(\boldsymbol{x}) \approx T^M(\boldsymbol{a},\boldsymbol{Y};\boldsymbol{x}) = a_j G(\boldsymbol{x},\boldsymbol{y}^j), \quad \boldsymbol{x}\in\overline{\Omega}, \tag{8}$$

where $\boldsymbol{a} = (a_1,\ldots,a_M)$ and $\boldsymbol{Y}$ is a $2M$-vector containing the coordinates of the source points $\boldsymbol{y}^j$, $j=1,\ldots,M$. On taking into account the definitions of the heat flux (2), the normal heat flux (5) and the fundamental solution (7) then the normal heat flux, through a curve defined by the outward unit normal vector $\boldsymbol{n}(\boldsymbol{x})$, can be approximated on the boundary Γ by

$$\Phi(\boldsymbol{x}) \approx \Phi^M(\boldsymbol{a},\boldsymbol{Y};\boldsymbol{x}) = a_j H(\boldsymbol{x},\boldsymbol{y}^j), \quad \boldsymbol{x}\in\Gamma, \tag{9}$$

where

$$\begin{aligned} H(\boldsymbol{x},\boldsymbol{y}) &= -n_i(\boldsymbol{x})K_{ij}\partial_j G(\boldsymbol{x},\boldsymbol{y})\exp(2\boldsymbol{\beta}\cdot\boldsymbol{x}) \\ &= -\frac{\exp(\boldsymbol{\beta}\cdot\boldsymbol{r})}{2\pi\sqrt{\det\mathbb{K}}}\left(\frac{\kappa}{R}(\boldsymbol{n}(\boldsymbol{x})\cdot\boldsymbol{r})K_1(\kappa R) + (\boldsymbol{n}(\boldsymbol{x})\cdot\boldsymbol{K}\boldsymbol{\beta})K_0(\kappa R)\right), \quad \boldsymbol{x}\in\Gamma,\ \boldsymbol{y}\in\mathbb{R}^2\setminus\overline{\Omega}, \end{aligned} \tag{10}$$

with K_1 the modified Bessel function of second kind of order one.

If N collocation points $\boldsymbol{x}^i$, $i=1,\ldots,N$, are chosen on the overspecified boundary Γ_1 of the domain Ω and the location of the source points y^j, $j=1,\ldots,M$, is set then Eqs. (8) and (9) recast as a system of $2N$ linear algebraic equations with M unknowns which can be generically written as

$$\mathbb{A}\boldsymbol{X} = \boldsymbol{F}, \tag{11}$$

where the MFS matrix $\mathbb{A}$, the unknown vector $\boldsymbol{X}$ and the right-hand side vector $\boldsymbol{F}$ are given by

$$\begin{aligned} &A_{ij} = G(\boldsymbol{x}^i,\boldsymbol{y}^j), \quad A_{N+ij} = H(\boldsymbol{x}^i,\boldsymbol{y}^j), \quad X_j = a_j, \\ &F_i = T(\boldsymbol{x}^i), \quad F_{N+i} = \Phi(\boldsymbol{x}^i), \quad i=1,\ldots,N, \quad j=1,\ldots,M. \end{aligned} \tag{12}$$

It should be noted that in order to uniquely determine the solution $\boldsymbol{X}$ of the system of linear algebraic equations (11), i.e. the coefficients a_j, $j=1,\ldots,M$, in the approximations (8) and (9), the number N of boundary collocation points and the number M of source points must satisfy the inequality $M\leqslant 2N$. However, the system of linear algebraic equations (11) cannot be solved by direct methods, such as the least-squares method, since such an approach would produce a highly unstable solution. Most of the standard numerical methods cannot achieve a good accuracy in the solution of the system of linear algebraic equations (11) due to the large value of the condition number of the matrix $\mathbb{A}$ which increases dramatically as the number of boundary collocation points and source points increases. It should be mentioned that for inverse problems, the resulting systems of linear algebraic equations are ill-conditioned, even if other well-known numerical methods (FDM, FEM or BEM) are employed. Although the MFS system of linear

algebraic equations (11) is ill-conditioned even when dealing with direct problems, the MFS has no longer this disadvantage in comparison with other numerical methods and, in addition, it preserves its advantages, such as the lack of any mesh, the high accuracy of the numerical results, etc.

3.1. Tikhonov regularization method

In our study, we only consider the Tikhonov regularization method, see Tikhonov and Arsenin (1986), since it is simple, non-iterative and it provides an explicit solution, see Eq. (16) below. In addition, it is feasible to apply the Tikhonov regularization method to large systems of equations unlike the singular value decomposition which may become prohibitive for such problems, see Hansen (2001). For other regularization techniques used for solving such ill-conditioned problems, we refer the reader to Hansen (1998).

The Tikhonov regularized solution to the system of linear algebraic equations (11) is given by

$$\boldsymbol{X}_\lambda : \mathscr{T}_\lambda(\boldsymbol{X}_\lambda) = \min_{\boldsymbol{X}\in\mathbb{R}^M} \mathscr{T}_\lambda(\boldsymbol{X}), \tag{13}$$

where $\mathscr{T}_\lambda$ represents the kth order Tikhonov functional given by

$$\mathscr{T}_\lambda(\cdot) : \mathbb{R}^M \to [0,\infty), \quad \mathscr{T}_\lambda(\boldsymbol{X}) = \|\mathbb{A}\boldsymbol{X} - \boldsymbol{F}\|_2^2 + \lambda^2 \|\mathbb{R}^{(k)}\boldsymbol{X}\|_2^2, \tag{14}$$

the matrix $\mathbb{R}^{(k)} \in \mathbb{R}^{(M-k)\times M}$ induces a $\mathscr{C}^k$-constraint on the solution $\boldsymbol{X}$ and $\lambda > 0$ is the regularization parameter to be chosen. For example, in the case of the zeroth-, first- and second-order Tikhonov regularization method the matrix $\mathbb{R}^{(k)}$, i.e. $k = 0, 1, 2$, is given by

$$\mathbb{R}^{(0)} = \begin{bmatrix} 1 & 0 & \dots & 0 \\ 0 & 1 & \dots & 0 \\ \vdots & \vdots & \ddots & \vdots \\ 0 & 0 & \dots & 1 \end{bmatrix} \in \mathbb{R}^{M\times M}, \quad \mathbb{R}^{(1)} = \begin{bmatrix} -1 & 1 & 0 & \dots & 0 \\ 0 & -1 & 1 & \dots & 0 \\ \vdots & \vdots & \ddots & \ddots & \vdots \\ 0 & 0 & \dots & -1 & 1 \end{bmatrix} \in \mathbb{R}^{(M-1)\times M},$$

$$\mathbb{R}^{(2)} = \begin{bmatrix} 1 & -2 & 1 & 0 & \dots & 0 \\ 0 & 1 & -2 & 1 & \dots & 0 \\ \vdots & \vdots & \ddots & \ddots & \ddots & \vdots \\ 0 & 0 & \dots & 1 & -2 & 1 \end{bmatrix} \in \mathbb{R}^{(M-2)\times M}. \tag{15}$$

Solving $\nabla\mathscr{T}_\lambda(\boldsymbol{X}) = 0$ for $\boldsymbol{X} \in \mathbb{R}^M$, we obtain that the Tikhonov regularized solution, $\boldsymbol{X}_\lambda$, of the problem (13) is given as the solution of the regularized equation

$$\left(\mathbb{A}^{\mathrm{T}}\mathbb{A} + \lambda^2 \mathbb{R}^{(k)^{\mathrm{T}}}\mathbb{R}^{(k)}\right)\boldsymbol{X} = \mathbb{A}^{\mathrm{T}}\boldsymbol{F}. \tag{16}$$

Since the simple least-squares solution, i.e. $\lambda = 0$, is completely dominated by contributions from data errors and rounding errors, it is necessary to use regularization when solving ill-conditioned systems of linear equations. By adding regularization we are able to damp out these contributions and maintain the norm $\|\mathbb{R}^{(k)}\boldsymbol{X}\|_2$ to be of reasonable size.

3.2. Choice of the regularization parameter

The choice of the regularization parameter in Eq. (16) is crucial for obtaining a stable solution and this is discussed next. If too much regularization, or damping, i.e. λ^2 large, is imposed on the solution of Eq. (16) then it will not fit the given data $\boldsymbol{F}$ properly and the residual norm $\|\mathbb{A}\boldsymbol{X} - \boldsymbol{F}\|_2$ will be too large. If too little

regularization is imposed on the solution of Eq. (16), i.e. λ^2 small, then the fit will be good, but the solution will be dominated by the contributions from the data errors, and hence $\|\mathbb{R}^{(k)}\boldsymbol{X}\|_2$ will be too large. It is quite natural to plot the norm of the solution as a function of the norm of the residual parametrised by the regularization parameter λ, i.e. $\{\|\mathbb{A}\boldsymbol{X}_\lambda - \boldsymbol{F}\|_2, \|\mathbb{R}^{(k)}\boldsymbol{X}_\lambda\|_2, \lambda > 0\}$. Hence, the L-curve is really a trade-off curve between two quantities that both should be controlled and, according to the L-curve criterion, the optimal value λ_{opt} of the regularization parameter λ is chosen at the "corner" of the L-curve, see Hansen (1998, 2001).

As with every practical method, the L-curve has its advantages and disadvantages. There are two main disadvantages or limitations of the L-curve criterion. The first disadvantage is concerned with the reconstruction of very smooth exact solutions, see Tikhonov et al. (1998). For such solutions, Hanke (1996) showed that the L-curve criterion will fail, and the smoother the solution, the worse the regularization parameter λ computed by the L-curve criterion. However, it is not clear how often very smooth solutions arise in applications. The second limitation of the L-curve criterion is related to its asymptotic behaviour as the problem size M increases. As pointed out by Vogel (1996), the regularization parameter λ computed by the L-curve criterion may not behave consistently with the optimal parameter λ_{opt} as M increases. However, this ideal situation in which the same problem is discretised for increasing M may not arise so often in practice. Frequently the problem size M is fixed by the particular measurement setup given by N, and if a larger M is required then a new experiment must be undertaken since the inequality $M \leqslant 2N$ must be satisfied. Apart from these two limitations, the advantages of the L-curve criterion are its robustness and ability to treat perturbations consisting of correlated noise, for more details see Hansen (2001).

4. Numerical results and discussion

In order to present the performance of the MFS in conjunction with the zeroth-order Tikhonov regularization method, we solve the Cauchy problem (4) and (6) associated with two-dimensional anisotropic FGMs for three typical examples in both smooth and piecewise smooth geometries:

Example 1 (Square anisotropic FGM plate: 1D case). We consider the following analytical solutions for the temperature and normal heat flux:

$$\begin{aligned} T^{(\text{an})}(\boldsymbol{x}) &= T_0 \frac{1 - \exp\{-2(\beta_1 x_1 + \beta_2 x_2)\}}{1 - \exp\{-2(\beta_1 + \beta_2)\}}, \\ \Phi^{(\text{an})}(\boldsymbol{x}) &= -2\{n_1(\boldsymbol{x})(K_{11}\beta_1 + K_{12}\beta_2) + n_2(\boldsymbol{x})(K_{21}\beta_1 + K_{22}\beta_2)\} \frac{T_0}{1 - \exp\{-2(\beta_1 + \beta_2)\}}, \end{aligned} \tag{17}$$

in the square $\Omega = \{\boldsymbol{x} = (x_1, x_2) | 0 < x_1, x_2 < 1\}$, where $T_0 = 100.0$, $\beta_1 = -0.5$, $\beta_2 = 0.0$, $K_{11} = 5.0$, $K_{12} = K_{21} = 0.0$ and $K_{22} = 1.0$. Here $\Gamma_1 = \{\boldsymbol{x} \in \Gamma | x_1 = 1, 0 \leqslant x_2 \leqslant 1\} \cup \{\boldsymbol{x} \in \Gamma | 0 \leqslant x_1 \leqslant 1, x_2 = 1\}$ and $\Gamma_2 = \{\boldsymbol{x} \in \Gamma | x_1 = 0, 0 \leqslant x_2 < 1\} \cup \{\boldsymbol{x} \in \Gamma | 0 \leqslant x_1 < 1,\ x_2 = 0\}$.

Example 2 (Square anisotropic FGM plate: 2D case). We consider the same solution domain Ω, boundaries Γ_1 and Γ_2, and analytical solutions for the temperature and normal heat flux as in Example 1, with $T_0 = 100.0$, $\beta_1 = -0.5$, $\beta_2 = 0.2$, $K_{11} = 3.0$, $K_{12} = K_{21} = 0.0$ and $K_{22} = 1.0$.

Example 3 (Circular anisotropic FGM plate: 2D case). We consider similar analytical solutions for the temperature and normal heat flux as in the previous examples in the unit disk $\Omega = \{\boldsymbol{x} = (x_1, x_2) | x_1^2 + x_2^2 < 1\}$, where $T_0 = 10.0$, $\beta_1 = -0.5$, $\beta_2 = 0.3$, $K_{11} = 3.0$, $K_{12} = K_{21} = 0.0$ and $K_{22} = 2.0$. Here $\Gamma_1 = \{\boldsymbol{x} \in \Gamma | 0 \leqslant \theta(\boldsymbol{x}) \leqslant \pi\}$ and $\Gamma_2 = \{\boldsymbol{x} \in \Gamma | \pi < \theta(\boldsymbol{x}) < 2\pi\}$, where $\theta(\boldsymbol{x})$ is the angular polar coordinate of $\boldsymbol{x}$.

It should be noted that for the examples considered, the Cauchy data is available on a portion Γ_1 of the boundary Γ such that $\text{meas}(\Gamma_1) = \text{meas}(\Gamma)/2$. The Cauchy problems investigated in this study have been solved using a uniform distribution of both the boundary collocation points $\boldsymbol{x}^i$, $i = 1, \ldots, N$, and the source points $\boldsymbol{y}^j$, $j = 1, \ldots, M$, with the mention that the later were located on the boundary of the disk $\text{B}(0, R)$, where the radius $R > 0$ was chosen such that $\overline{\Omega} \subset \text{B}(0, R)$. Furthermore, the number of boundary collocation points was set to $N = 40$ for the Examples 1–3.

4.1. Stability of the method

In order to investigate the stability of the MFS, the temperature $T|_{\Gamma_1} = T^{(\text{an})}|_{\Gamma_1}$ has been perturbed as $\widetilde{T} = T + \delta T$, where δT is a Gaussian random variable with mean zero and standard deviation $\sigma = \max_{\Gamma_1} | T | \times (p_T/100)$, generated by the NAG subroutine G05DDF, and $p_T\%$ is the percentage of additive noise included in the input temperature data $T|_{\Gamma_1}$ in order to simulate the inherent measurement errors.

Fig. 1 presents the L-curves obtained for the Cauchy problem given by Example 1 using the zeroth-order Tikhonov regularization method, i.e. $k = 0$ in Eq. (14), to solve the MFS system (11), $M = 40$ source points, $R = 5.0$ and with various levels of noise added into the input temperature data. From this figure it can be seen that for each amount of noise considered the "corner" of the corresponding L-curve can be clearly determined and $\lambda = \lambda_{\text{opt}} = 10^{-5}$ and $\lambda = \lambda_{\text{opt}} = 10^{-4}$ for $p_T = 1$ and $p_T \in \{3, 5\}$, respectively.

In order to analyse the accuracy of the numerical results obtained, we consider the discretised L_2-norms on the underspecified boundary Γ_2 corresponding to the analytical temperature $T^{(\text{an})}$ and normal heat flux $\Phi^{(\text{an})}$, namely,

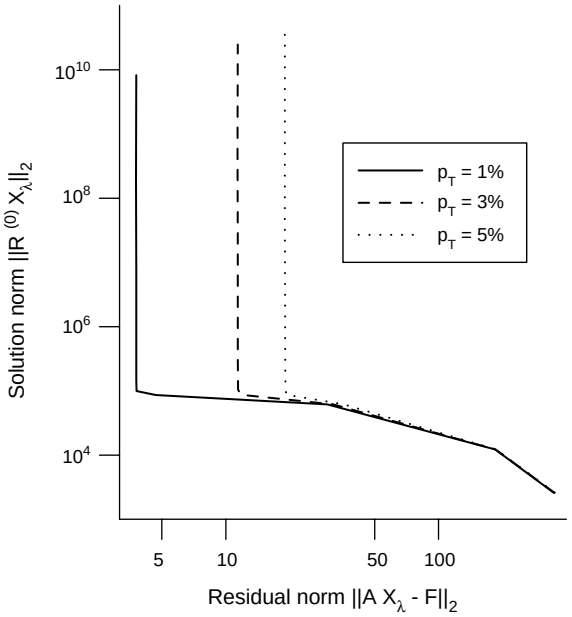

Fig. 1. The L-curves obtained for various levels of noise added into the temperature data $T|_{\Gamma_1}$, namely $p_T = 1\%$ (—), $p_T = 3\%$ (– –) and $p_T = 5\%$ (· · ·), with $M = 40$ source points, $N = 40$ boundary collocation points and $R = 5.0$ for Example 1.

$$\|T^{(\mathrm{an})}\|_2 = \sqrt{\frac{1}{L}\sum_{l=1}^{L}(T^{(\mathrm{an})}(\boldsymbol{x}^l))^2}, \quad \|\Phi^{(\mathrm{an})}\|_2 = \sqrt{\frac{1}{L}\sum_{l=1}^{L}(\Phi^{(\mathrm{an})}(\boldsymbol{x}^l))^2}, \tag{18}$$

where $\boldsymbol{x}^l$, $l = 1, \ldots, L$, are L uniformly distributed points on the boundary Γ_2. The absolute errors e_T and e_Φ can be defined as

$$e_T(\lambda, M, R) = \|T^{(\mathrm{an})} - T^{(\lambda)}\|_2, \quad e_\Phi(\lambda, M, R) = \|\Phi^{(\mathrm{an})} - \Phi^{(\lambda)}\|_2. \tag{19}$$

where $T^{(\lambda)}$ and $\Phi^{(\lambda)}$ are the numerical temperature and normal heat flux, respectively, obtained for the value λ of the regularization parameter and using M source points uniformly distributed on the boundary of the disk $B(0, R)$. Fig. 2(a) and (b) illustrate the accuracy errors e_T and e_Φ given by relation (19), as functions of the regularization parameter λ, obtained with various levels of noise added into the input temperature data $T|_{\Gamma_1}$ for the Cauchy problem given by Example 1. From these figures it can be seen that both errors e_T and e_Φ decrease as the level of noise added into the input temperature data decreases for all the regularization parameters λ and $e_T < e_\Phi$ for all the regularization parameters λ and a fixed amount p_T of noise added into the input temperature data, i.e. the numerical results obtained for the temperature are more accurate than those retrieved for the normal heat flux on the underspecified boundary Γ_2. Furthermore, by comparing Figs. 1 and 2, it can be seen, for various levels of noise, that the "corner" of the L-curve occurs at about the same value of the regularization parameter λ where the minimum in the accuracy errors e_T and e_Φ is attained. Hence the choice of the optimal regularization parameter λ_{opt} according to the L-curve criterion is fully justified. Similar results have been obtained for the Cauchy problems given by Examples 2 and 3 and therefore they are not presented here. It should be mentioned that, as expected, the errors in evaluating the temperature and normal heat flux on the underspecifed boundary Γ_2 are more sensitive to the noise added into the input flux data $\Phi|_{\Gamma_1}$ than to the noise added into the input temperature data $T|_{\Gamma_1}$, since the flux contains first-order derivatives of the temperature.

Fig. 3(a) and (b) illustrate the analytical and the numerical results for the temperature T on the underspecified boundary $x_1 = 0$ and the normal heat flux Φ on the underspecified boundary $x_2 = 0$, respectively,

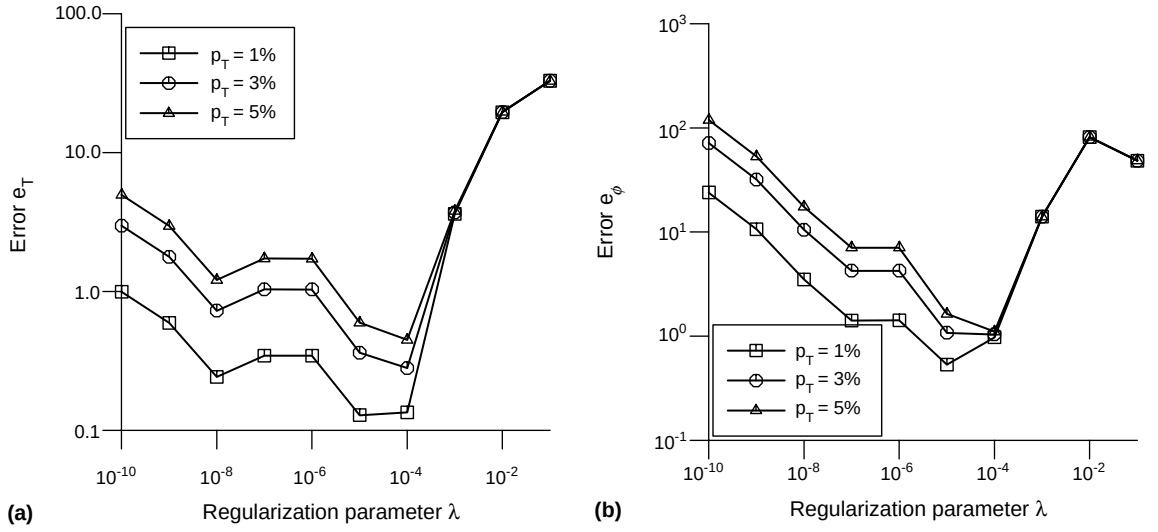

Fig. 2. The accuracy errors (a) e_T, and (b) e_Φ, as functions of the regularization parameter λ, obtained for various levels of noise added into the temperature data $T|_{\Gamma_1}$, namely $p_T = 1\%$ (□), $p_T = 3\%$ (○) and $p_T = 5\%$ (△), with $M = 40$ source points, $N = 40$ boundary collocation points and $R = 5.0$ for Example 1.

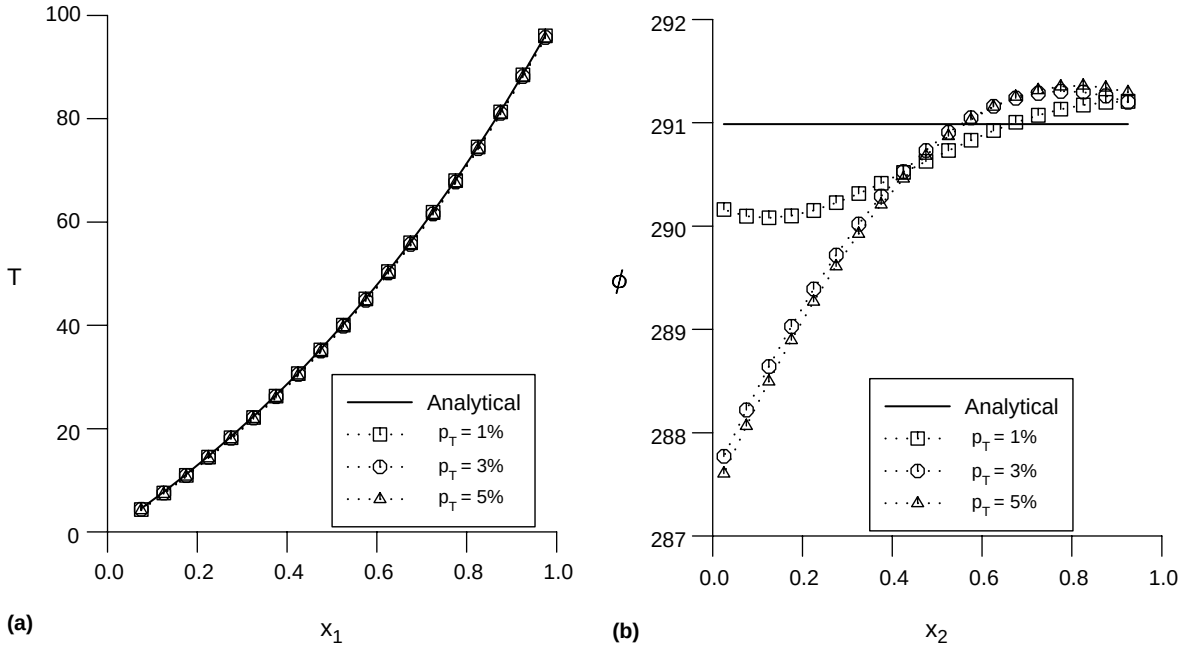

Fig. 3. (a) The analytical $T^{(\mathrm{an})}$ (—) and the numerical $T^{(\lambda)}$ temperatures on the underspecified boundary $x_2 = 0$, and (b) the analytical $\Phi^{(\mathrm{an})}$ (—) and the numerical $\Phi^{(\lambda)}$ fluxes on the underspecified boundary $x_1 = 0$, retrieved using $M = 40$ source points, $N = 40$ boundary collocation points, $R = 5.0$, $\lambda = \lambda_{\mathrm{opt}}$ and various levels of noise added into the temperature data $T|_{\Gamma_1}$, namely $p_T = 1\%$ ($\cdots\Box\cdots$), $p_T = 3\%$ ($\cdots\bigcirc\cdots$) and $p_T = 5\%$ ($\cdots\triangle\cdots$), for Example 1.

obtained using the optimal regularization parameter $\lambda = \lambda_{\mathrm{opt}}$ chosen according to the L-curve criterion, $M = 40$ source points, $R = 5.0$ and various levels of noise added into the input tempearture data $T|_{\Gamma_1}$, namely $p_T \in \{1, 3, 5\}$, for the Cauchy problem given by Example 1. From these figures we can conclude that the numerical solutions retrieved for Example 1 are stable with respect to the amount of noise p_T added into the input temperature data $T|_{\Gamma_1}$. Moreover, a similar conclusion can be drawn from Figs. 4 and 5 which present the numerical results for the temperature T and normal heat flux Φ on the underspecified boundary Γ_2 in comparison with their analytical values, obtained using $\lambda = \lambda_{\mathrm{opt}}$ chosen according to the L-curve criterion, $M = 40$ source points, $R = 5.0$ and various levels of noise added into the input temperature data $T|_{\Gamma_1}$, namely $p_T \in \{1, 3, 5\}$, for the Cauchy problems given by Examples 2 and 3, respectively.

4.2. Convergence and accuracy of the method

In order to investigate the influence of the number M of source points on the accuracy and stability of the numerical solutions for the temperature and normal heat flux on the underspecified boundary Γ_2, we set $R = 5.0$ and $p_T = 5$ for the Cauchy problem given by Example 2. Although not presented here, it should be noted that similar results have been obtained for the Cauchy problems given by the other examples considered in this study. To do so, we define the normalised errors E_T and E_Φ for the temperature and the normal heat flux, respectively, as

$$E_T(M,R) = \frac{e_T(\lambda_{\mathrm{opt}}, M, R)}{\|T^{(\mathrm{an})}\|_2}, \quad E_\Phi(M,R) = \frac{e_\Phi(\lambda_{\mathrm{opt}}, M, R)}{\|\Phi^{(\mathrm{an})}\|_2}, \tag{20}$$

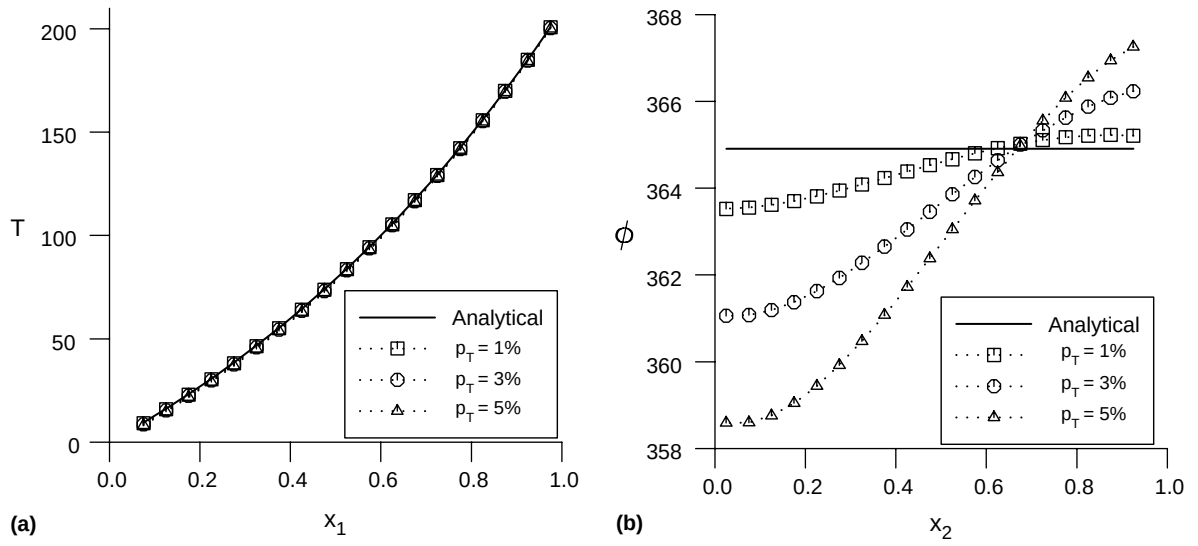

Fig. 4. (a) The analytical $T^{(\mathrm{an})}$ (—) and the numerical $T^{(\lambda)}$ temperatures on the underspecified boundary $x_2 = 0$, and (b) the analytical $\Phi^{(\mathrm{an})}$(—) and the numerical $\Phi^{(\lambda)}$ fluxes on the underspecified boundary $x_1 = 0$, retrieved using $M = 40$ source points, $N = 40$ boundary collocation points, $R = 5.0$, $\lambda = \lambda_{\mathrm{opt}}$ and various levels of noise added into the temperature data $T|_{\Gamma_1}$, namely $p_T = 1\%$ ($\cdots\square\cdots$), $p_T = 3\%$ ($\cdots\bigcirc\cdots$) and $p_T = 5\%$ ($\cdots\triangle\cdots$), for Example 2.

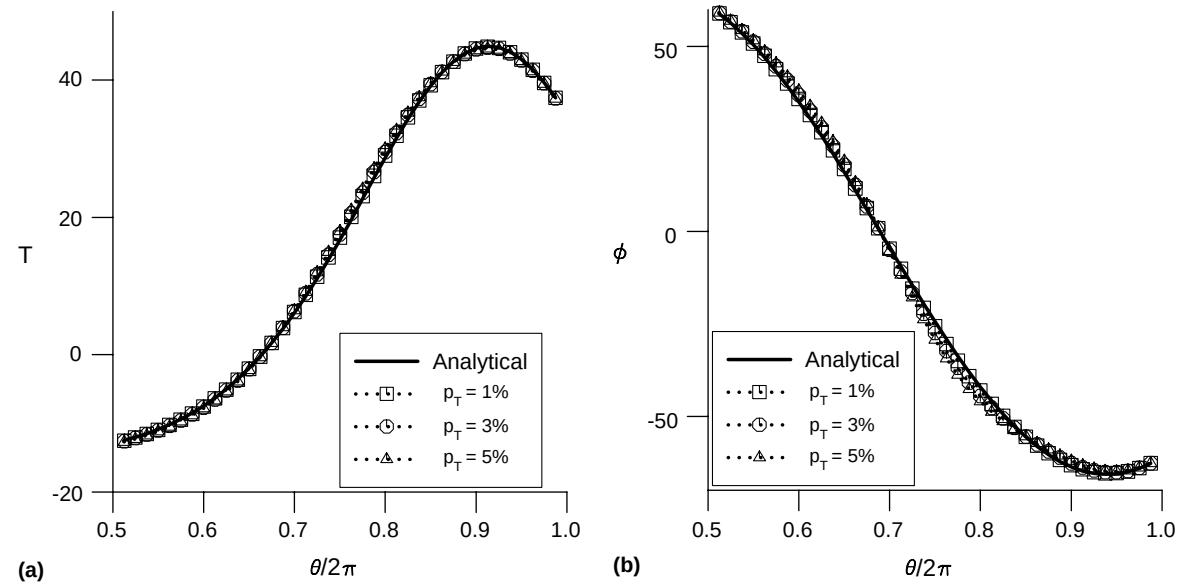

Fig. 5. (a) The analytical $T^{(\mathrm{an})}$ (—) and the numerical $T^{(\lambda)}$ temperatures, and (b) the analytical $\Phi^{(\mathrm{an})}$ (—) and the numerical $\Phi^{(\lambda)}$ fluxes, retrieved on the underspecified boundary Γ_2 with $M = 40$ source points, $N = 40$ boundary collocation points, $R = 5.0$, $\lambda = \lambda_{\mathrm{opt}}$ and various levels of noise added into the temperature data $T|_{\Gamma_1}$, namely $p_T = 1\%$ ($\cdots\square\cdots$), $p_T = 3\%$ ($\cdots\bigcirc\cdots$) and $p_T = 5\%$ ($\cdots\triangle\cdots$), for Example 3.

where $e_T(\lambda_{\text{opt}}, M, R)$ and $e_\Phi(\lambda_{\text{opt}}, M, R)$ are given by Eq. (19) with $\lambda = \lambda_{\text{opt}}$, and $\|T^{(\text{an})}\|_2$ and $\|\Phi^{(\text{an})}\|_2$ are the discretised L_2-norms of the temperature and normal heat flux, respectively, defined by relation (18).

In Fig. 6(a) and (b) we present the normalised errors E_T and E_Φ for the Example 2, respectively, as functions of the number M of source points, obtained using $\lambda = \lambda_{\text{opt}}$ given by the L-curve criterion. It can be seen from these figures that both normalised errors tend to zero as the number M of source points increases, with the mention that E_Φ increases slightly for $M \geqslant 20$, and, in addition, these errors do not vary substantially for $M \geqslant 10$. These results indicate the fact that accurate numerical solutions for the temperature and the normal heat flux on the underspecified boundary Γ_2 can be obtained using a relatively small number M of source points.

Next, we analyse the convergence of the numerical method proposed with respect to the position of the source points. To do so, we set $M = 40$ and $p_T = 5$ for the Cauchy problem given by Example 1, while at the same time varying the radius $R \in [R_{\min}, R_{\max}]$. Fig. 7(a) and (b) illustrate the normalised errors E_T and E_Φ defined by relation (20) for Example 1, respectively, as functions of R, obtained using $\lambda = \lambda_{\text{opt}}$ given by the L-curve criterion, $R_{\min} = 1.5$ and $R_{\max} = 10$. From these figures it can be seen that the larger is the distance from the source points to the boundary of the solution domain Ω, i.e. the larger is R, the better the accuracy in the numerical temperature and normal heat flux. It should be noted that the value $R = 6$ was found to be sufficiently large such that any further increase of the distance between the source points and the boundary Γ did not significantly improve the accuracy of the numerical solutions for the examples tested in this paper.

It is interesting to mention that, in practice both accuracy errors e_T and e_Φ deteriorate if $R_{\max}$ is very large and this is contrary with some of the theoretical results available in the literature. This feature of the MFS can be noticed from Fig. 8(a) and (b) which illustrate the behaviour of the accuracy errors e_T and e_Φ, respectively, obtained using $\lambda = \lambda_{\text{opt}}$ given by the L-curve criterion, $M = 40$ source points, $R_{\min} \leqslant R \leqslant R_{\max}$, $R_{\min} = 1.5$ and $R_{\max} = 50$. It can be seen from these figures that both errors e_T and e_Φ start increasing for $R \geqslant 16$. However, the optimal choice of R still remains an open problem, as pointed out by Katsurada and Okamoto (1996), and it requires further research.

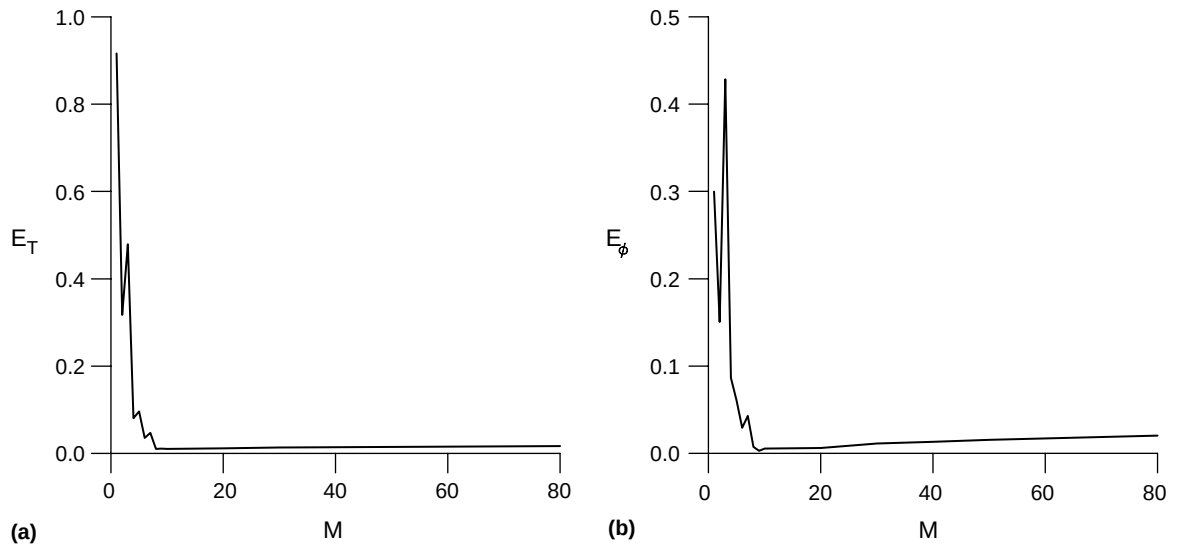

Fig. 6. The normalised accuracy errors (a) E_T, and (b) E_Φ, obtained with $N = 40$ boundary collocation points, $R = 5.0$, $\lambda = \lambda_{\text{opt}}$ and $p_T = 5\%$ for Example 2, as functions of the number M of source points.

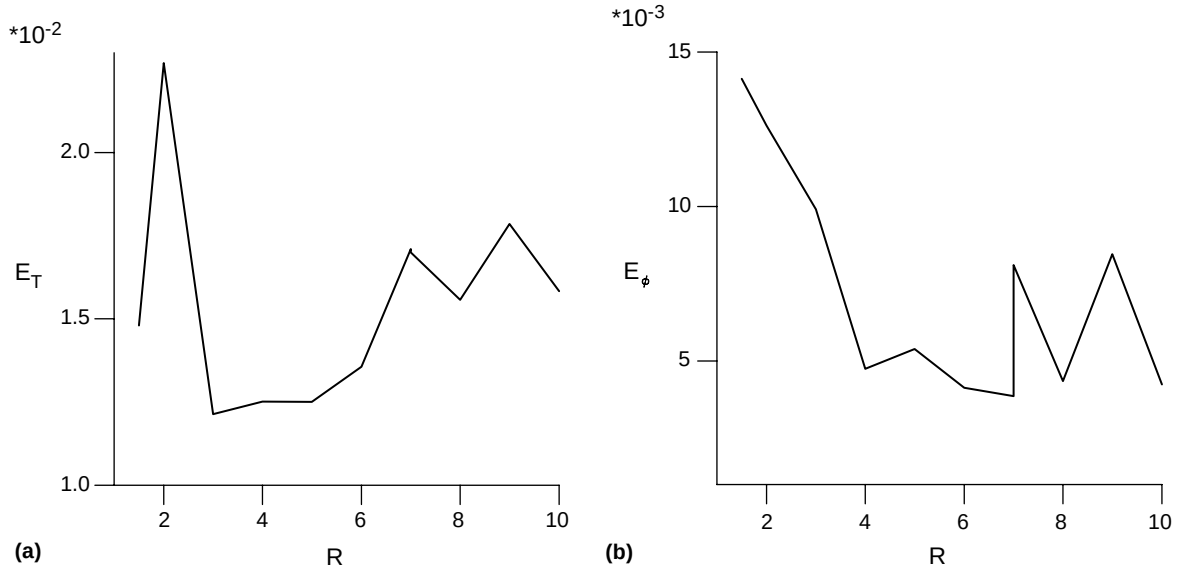

Fig. 7. The normalised accuracy errors (a) E_T, and (b) E_Φ, obtained with $M = 40$ source points, $N = 40$ boundary collocation points, $\lambda = \lambda_{\text{opt}}$ and $p_T = 5\%$ for Example 1, as functions of the distance R between the source points and the boundary Γ of the solution domain Ω.

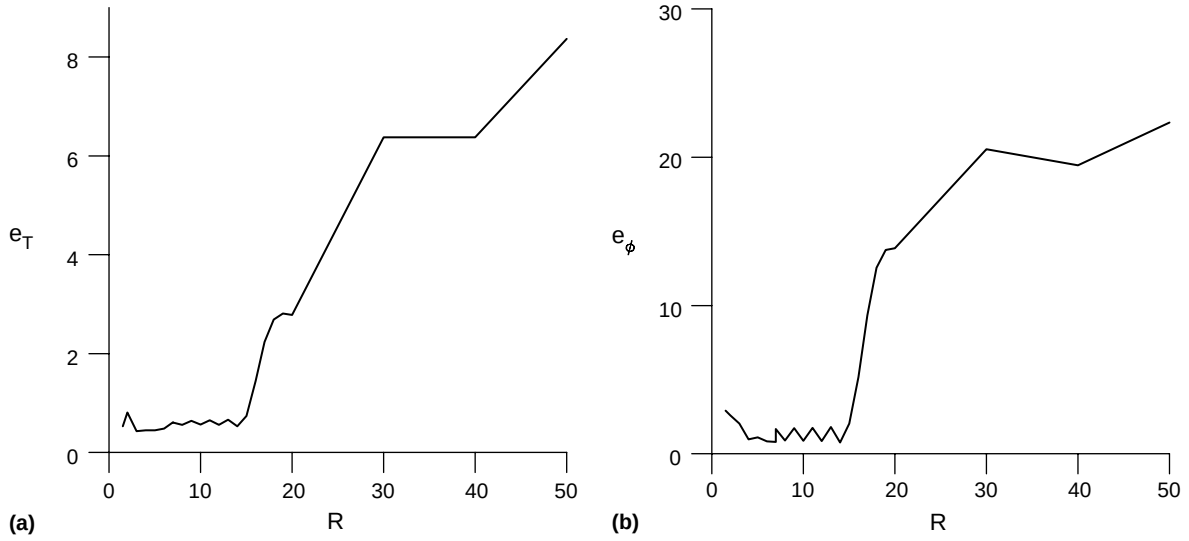

Fig. 8. The accuracy errors (a) e_T, and (b) e_Φ, obtained with $M = 40$ source points, $N = 40$ boundary collocation points, $\lambda = \lambda_{\text{opt}}$ and $p_T = 5\%$ for Example 1, as functions of the distance R between the source points and the boundary Γ of the solution domain Ω.

5. Conclusions

In this paper, the Cauchy problem associated with two-dimensional anisotropic FGMs has been investigated by employing the MFS. The resulting ill-conditioned system of linear algebraic equations has been

regularized by using the zeroth-order Tikhonov regularization method, while the choice of the optimal regularization parameter was based on the L-curve criterion. Three examples involving both smooth and piecewise smooth geometries have been analysed. The numerical results obtained show that the proposed method is convergent with respect to increasing the number of source points and the distance from the source points to the boundary of the solution domain up to a threshold value (which is "large" from the numerical point of view) and stable with respect to decreasing the amount of noise added into the input data. Moreover, the method is efficient and easy to adapt to irregular domains.

Acknowledgement

The author would like to thank Prof. D.B. Ingham, Dr. L. Elliott and Dr. D. Lesnic from the Department of Applied Mathematics at the University of Leeds for all their encouragement in performing this research work. The constructive suggestions made by the referees are gratefully acknowledged.

References

Berger, J.R., Karageorghis, A., 1999. The method of fundamental solutions for heat conduction in layered materials. International Journal for Numerical Methods in Engineering 45, 1681–1694.

Berger, J.R., Karageorghis, A., 2001. The method of fundamental solutions for layered elastic materials. Engineering Analysis with Boundary Elements 25, 877–886.

Berger, J.R., Martin, P.A., Mantič, V., Gray, L.J., in press. Fundamental solutions for steady-state heat transfer in an exponentially-graded material. Zeitschrift für Angewandte Mathematik und Physik.

Clements, D.L., Budhi, W.S., 1999. A boundary element method for the solution of a class of steady-state problems for anisotropic media. Heat Transfer 121, 462–465.

Desplat, J.L., 1996. Recent developments on oxygenated thermionic energy converter-overview. In: Yamanouochi, M., Koizumi, M., Hirai, T., Shiota, I. (Eds.), Proceedings of the Fourth International Symposium on Functionally Graded Materials, Tsukuba City, Japan, pp. 209–214.

Fairweather, G., Karageorghis, A., 1998. The method of fundamental solutions for elliptic boundary value problems. Advances in Computational Mathematics 9, 69–95.

Gray, L.J., Kaplan, T., Richardson, J.D., Paulino, G.H., 2003. Green's functions and boundary integral equations for functionally graded materials: heat conduction. Journal of Applied Mechanics 70, 543–549.

Hadamard, J., 1923. Lectures on Cauchy Problem in Linear Partial Differential Equations. Oxford University Press, London.

Hanke, M., 1996. Limitations of the L-curve method in ill-posed problems. BIT 36, 287–301.

Hansen, P.C., 1998. Rank-deficient and Discrete Ill-posed Problems: Numerical Aspects of Linear Inversion. SIAM, Philadelphia.

Hansen, P.C., 2001. The L-curve and its use in the numerical treatment of inverse problems. In: Johnston, P. (Ed.), Computational Inverse Problems in Electrocardiology. WIT Press, Southampton, pp. 119–142.

Hào, D.N., Lesnic, D., 2000. The Cauchy problem for Laplace's equation via the conjugate gradient method. IMA Journal of Applied Mathematics 65, 199–217.

Hirano, T., Teraki, J., Yamada, T., 1990. On the design of functionally graded materials. In: Yamanouochi, M., Koizumi, M., Hirai, T., Shiota, I. (Eds.), Proceedings of the First International Symposium on Functionally Graded Materials. Sendai, Japan, pp. 5–10.

Igari,T., Notomi, A., Tsunoda, H., Hida, K., Kotoh, T., Kunishima, S., 1990. Material properties of functionally graded material for fast breeder reactor. In: Yamanouochi, M., Koizumi, M., Hirai, T., Shiota, I. (Eds.), Proceedings of the First International Symposium on Functionally Graded Materials. Sendai, Japan, pp. 209–214.

Ingham, D.B., Yuan, Y., 1994. Boundary element solutions of the steady state, singular, inverse heat transfer equation. International Journal of Heat and Mass Transfer 37, 273–280.

Karageorghis, A., 2001. The method of fundamental solutions for the calculation of the eigenvalues of the Helmholtz equation. Applied Mathematics Letters 14, 837–842.

Karageorghis, A., Fairweather, G., 1987. The method of fundamental solutions for the numerical solution of the biharmonic equation. Journal of Computational Physics 69, 434–459.

Katsurada, M., Okamoto, H., 1996. The collocation points of the fundamental solution method for the potential problem. Computers and Mathematics with Applications 31, 123–137.

Koike, Y., 1992. Graded index and single mode polymer optical fibres. In: Chiang, L.Y., Garito, A.G., Sandman, D.J. (Eds.), Electrical, Optical and Magnetic Properties of Organic Solid State Materials, Materials Research Proceedings, vol. 247. MRS, Pittsburg, PA, p. 817.

Kupradze, V.D., Aleksidze, M.A., 1964. The method of functional equations for the approximate solution of certain boundary value problems. USSR Computational Mathematics and Mathematical Physics 4, 82–126.

Lesnic, D., Elliott, L., Ingham, D.B., 1997. An iterative boundary element method for solving numerically the Cauchy problem for the Laplace equation. Engineering Analysis with Boundary Elements 20, 123–133.

Marin, L., A meshless method for solving the Cauchy problem in three-dimensional elastostatics. Computers and Mathematics with Applications, in press.

Marin, L., A meshless method for the numerical solution of the Cauchy problem associated with three-dimensional Helmholtz-type equations. Applied Mathematics and Computation, in press.

Marin, L., Lesnic, D., 2004. The method of fundamental solutions for the Cauchy problem in two-dimensional linear elasticity. International Journal of Solids and Structures 41, 3425–3438.

Marin, L., Lesnic, D., 2005. The method of fundamental solutions for the Cauchy problem associated with two-dimensional Helmholtz-type equations. Computers and Structures 83, 267–278.

Marin, L., Elliott, L., Heggs, P.J., Ingham, D.B., Lesnic, D., Wen, X., 2003a. An alternating iterative algorithm for the Cauchy problem associated to the Helmholtz equation. Computer Methods in Applied Mechanics and Engineering 192, 709–722.

Marin, L., Elliott, L., Heggs, P.J., Ingham, D.B., Lesnic, D., Wen, X., 2003b. Conjugate gradient-boundary element solution to the Cauchy problem for Helmholtz-type equations. Computational Mechanics 31, 367–377.

Mera, N.S., Elliott, L., Ingham, D.B., Lesnic, D., 2000. The boundary element solution of the Cauchy steady heat conduction problem in an anisotropic medium. International Journal for Numerical Methods in Engineering 49, 481–499.

Mera, N.S., Elliott, L., Ingham, D.B., Lesnic, D., 2002. An iterative algorithm for singular Cauchy problems for the steady state anisotropic heat conduction equation. Engineering Analysis with Boundary Elements 26, 157–168.

Oonishi, H., Noda, T., Ito, S., Kohda, A., Yamamoto, H., Tsuji, E., 1994. Effect of hydroxyapatite coating on boned growth into porous titanium alloy implants under loaded conditions. Journal of Applied Biomaterials 5, 23–27.

Osaka, T., Matsubara, H., Homma, T., Mitamura, S., Noda, K., 1990. Microstructural study of electroless-plated CoNiReP/NiMoP double-layered media for perpendicular magnetic recording. Japanese Journal of Applied Physics 29, 1939–1943.

Poullikkas, A., Karageorghis, A., Georgiou, G., 1998a. Methods of fundamental solutions for harmonic and biharmonic boundary value problems. Computational Mechanics 21, 416–423.

Poullikkas, A., Karageorghis, A., Georgiou, G., 1998b. The method of fundamental solutions for inhomogeneous elliptic problems. Computational Mechanics 22, 100–107.

Poullikkas, A., Karageorghis, A., Georgiou, G., 2001. The numerical solution of three-dimensional Signorini problems with the method of fundamental solutions. Engineering Analysis with Boundary Elements 25, 221–227.

Poullikkas, A., Karageorghis, A., Georgiou, G., 2002. The numerical solution for three-dimensional elastostatics problems. Computers and Structures 80, 365–370.

Ramachandran, P.A., 2002. Method of fundamental solutions: singular value decomposition analysis. Communications in Numerical Methods in Engineering 18, 789–801.

Suresh, S., Mortensen, A., 1998. Fundamentals of Functionally Graded Materials. IOM Communications Ltd., London.

Tani, J., Liu, G.R., 1993. Surface waves in functionally graded piezoelectric plates. JSME International Journal Series A (Mechanics and Material Engineering) 36, 152–155.

Tikhonov, A.N., Arsenin, V.Y., 1986. Methods for Solving Ill-posed Problems. Nauka, Moscow.

Tikhonov, A.N., Leonov, A.S., Yagola, A.G., 1998. Nonlinear Ill-posed Problems. Chapman & Hall, London.

Vogel, C.R., 1996. Non-convergence of the L-curve regularization parameter selection method. Inverse Problems 12, 535–547.

Watanabe, Y., Nakamura, Y., Fukui, Y., Nakanishi, K., 1993. A magnetic-functionally graded material manufactured with deformation-induced martensitic transformation. Journal of Material Science Letters 12, 326–328.